

InGaAs/InP DHBTs using MOCVD Selective Emitter Regrowth

P. Choudhary¹, C-Y. Huang¹, J.C. Rode¹, H.W. Chiang², M.J.W. Rodwell¹

¹ECE Department, University of California, Santa Barbara, USA, ²Intel PTD, Portland, OR 97006, prateek[dot]pc[at]gmail[dot]com

By scaling [1] semiconductor thicknesses, lithographic dimensions, and contact resistivities [2], the bandwidth of InGaAs/InP DHBTs has reached 550/1100 GHz f_{τ}/f_{\max} at the 128nm node [3]. Two difficulties are faced in scaling to the higher-bandwidth 64nm and 32nm nodes. Auger recombination in the $\sim 10^{20}/\text{cm}^3$ -doped base, and electron transport from the emitter to the base contacts [4] both cause DC current gain β to decrease with scaling. Though $< 2 \Omega\text{-}\mu\text{m}^2$ base contact resistivity, necessary [1] for $> 1.5\text{THz } f_{\max}$, has been demonstrated on test structures [2], obtaining such resistivity in processed HBTs is difficult because of process-induced surface contamination. Because the base is only $\sim 10\text{-}15\text{nm}$ thick [1] at the 64nm and 32nm nodes, it is difficult to remove surface contamination by etching, or to penetrate through it with Pd/Pt alloyed contacts without consuming the entire base thickness. If, as with Si/SiGe HBTs [5], the InP HBT has a thin P- intrinsic base under the emitter but a thicker P+ extrinsic base under the contacts, then Auger recombination is reduced, increasing β , the P+/P- junction field inhibits electron transport to the base [4], again increasing β , and the P+ extrinsic base can be made sufficiently thick for surface contaminants to be removed by etching or penetrated by alloyed contacts, reducing contact resistivity and increasing f_{\max} . Such devices can be formed by base [6] or emitter regrowth [7]. Here we report a self-aligned process to form such devices in InGaAs/InP by emitter regrowth by MOCVD. We show initial DC results.

Fabrication (fig. 1) starts with deposition of a SiO₂ mask the p-InGaAs base. Emitter regrowth windows are etched into the oxide, and the exposed base is digitally etched to thin the intrinsic base. The emitter, 15nm InP ($5 \cdot 10^{18} \text{ cm}^{-3}$), 15nm InP ($4 \cdot 10^{19} \text{ cm}^{-3}$), and 20nm InGaAs ($4 \cdot 10^{19} \text{ cm}^{-3}$), was then regrown at 600 C in a Thomas Swan 2" MOCVD reactor using TBP, TBAs, TMI, and TMG sources. During regrowth, hydrogen passivates the carbon base dopant [8]; the hydrogen is removed by a 500 C anneal [8]. Emitter metal is lifted off, the oxide mask removed, the base mesa defined by wet-etching, the base and collector contacts deposited, and the collector mesas isolated. The emitter metal overhang on the oxide allows for self aligned base metal deposition. [4] proposes a more complex, fully-self-aligned process.

Fig. 2a shows a TEM image of a 500nm width regrown emitter and its contact. Fig. 2b shows the emitter-base junction, the 10 nm intrinsic base and the 15nm extrinsic base. The total base is graded from $9\text{-}5 \cdot 10^{19} \text{ cm}^{-3}$ doping and is 25nm thick. The present devices suffer from high base-collector leakage from penetration of the contact metal through the base at the junction edges (fig. 2c). The base contact resistivity is also high. These process difficulties are unrelated to the base emitter regrowth process and are readily resolved. Fig 3. shows $\log(I)\text{-}V$ characteristics of the base-emitter junction. The Gummel characteristics (fig. 4) show $\beta \sim 11$ at $V_{\text{CB}} = 0 \text{ V}$. As the fabrication and regrowth processes are resolved, MOCVD emitter regrowth may provide a means to decouple the parameters of the HBT intrinsic and extrinsic base, thereby permitting high DC current gain and low base contact resistivity in highly scaled InP HBTs.

References:

- [1] M. J. W. Rodwell, M. Le, B. Brar, "InP bipolar ICs: Scaling roadmaps, frequency limits, manufacturable technologies", IEEE Proceedings, Vol. 92, No. 2, pp 271-286, 2008.
- [2] A. Baraskar, A.C. Gossard, M.J.W. Rodwell, "Lower limits to metal-semiconductor contact resistance: Theoretical models and experimental data", Journal of Applied Physics 114 (15), 154516.
- [3] M. Urteaga, R. Pierson, P. Rowell, V. Jain, E. Lobisser, M.J.W. Rodwell, "130nm InP DHBTs with $f_{\tau} > 0.52 \text{ THz}$ and $f_{\max} > 1.1 \text{ THz}$ ", 2011 IEEE Device Research Conference, June, Santa Barbara.
- [4] H.-W. Chiang, J. C. Rode, P. Choudhary, and M. J. W. Rodwell, "Optimization of direct current performance in terahertz InGaAs/InP double-heterojunction bipolar transistors," J. Appl. Phys., vol. 116, no. 16, pp. 164509–164509–6, Oct. 2014.
- [5] J.J. Pekarik *et al.*, "A 90nm SiGe BiCMOS Technology for mm-wave and high-performance analog applications", 2014 IEEE Bipolar/BiCMOS Circuits and Technology Meeting (BCTM), Sept. 28-Oct. 1, Coronado, CA.
- [6] H. Shimawaki, Y. Amamiya, N. Furuhashi, and K. Honjo, "High- f_{\max} AlGaAs/InGaAs and AlGaAs/GaAs HBT's with p+/p regrown base contacts," IEEE Trans. Electron Devices, vol. 42, no. 10, pp. 1735–1744, Oct. 1995.
- [7] D. W. Scott, Y. Wei, Y. Dong, A. C. Gossard, and M. J. Rodwell, "A 183 GHz f_{τ} and 165 GHz f_{\max} regrown-emitter DHBT with abrupt InP emitter," IEEE Electron Device Lett., vol. 25, no. 6, pp. 360–362, Jun. 2004.
- [8] N. Watanabe, S. Yamahata, and T. Kobayashi, "Hydrogen removal by annealing from C-doped InGaAs grown on InP by metalorganic chemical vapor deposition," J. Cryst. Growth, vol. 200, no. 3–4, pp. 599–602, Apr. 1999.

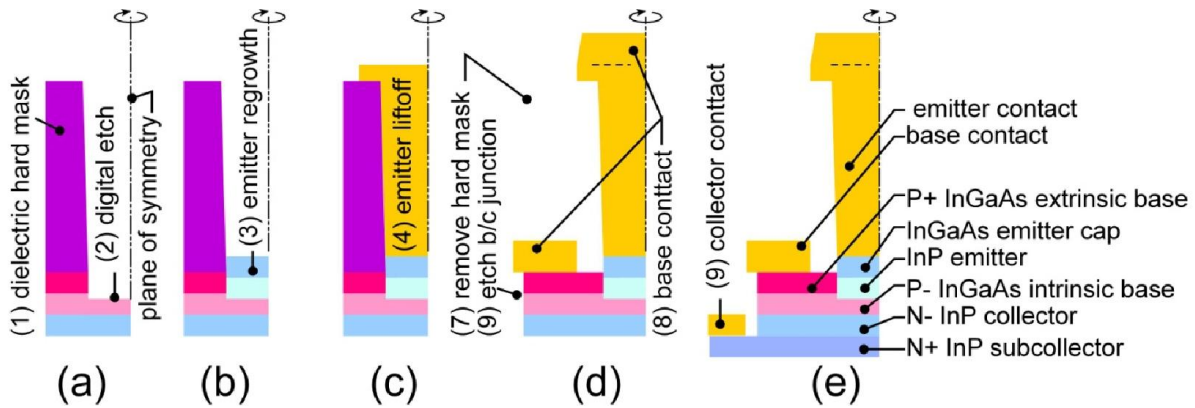


Fig. 1: HBT process flow: A regrowth window is defined and the semiconductor etched (a), the emitter regrown (b), the emitter contact deposited (c), the base mesa etched and the base and collector contacts deposited (d,e).

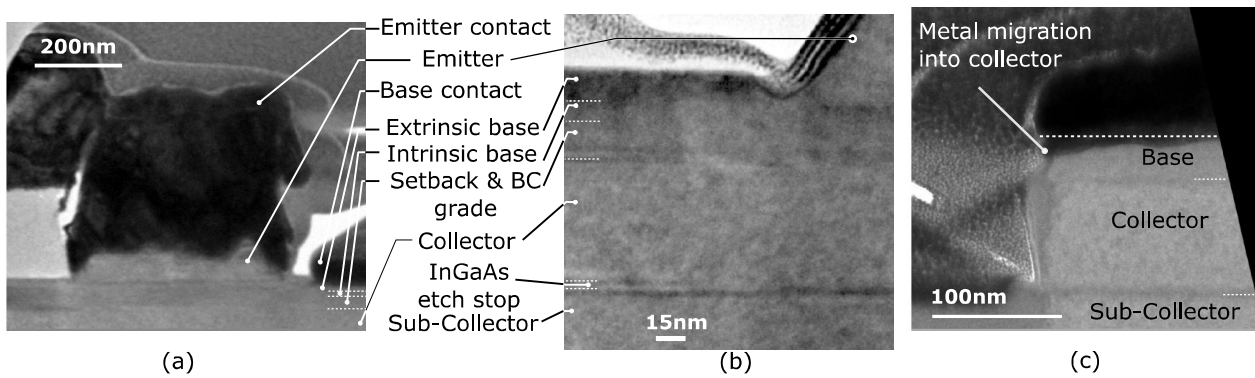


Fig. 2: TEM image showing cross section (a), the 500nm emitter and base contact to its right. The left base contact is further due to misalignment, and is not shown for space considerations (b), the base-emitter junction, and the intrinsic and extrinsic base (c), the base mesa edge. Base metal penetration at the junction edge on this sample causes high leakage.

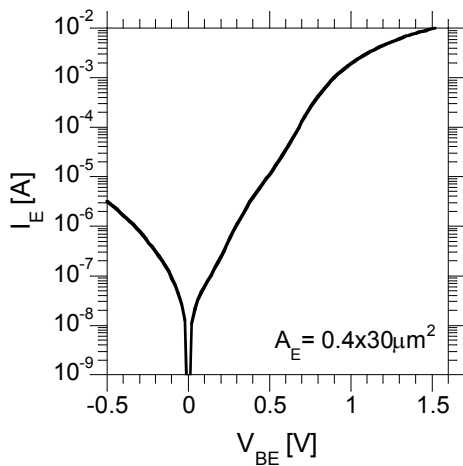


Fig.3: DC characteristics of the base-emitter junction.

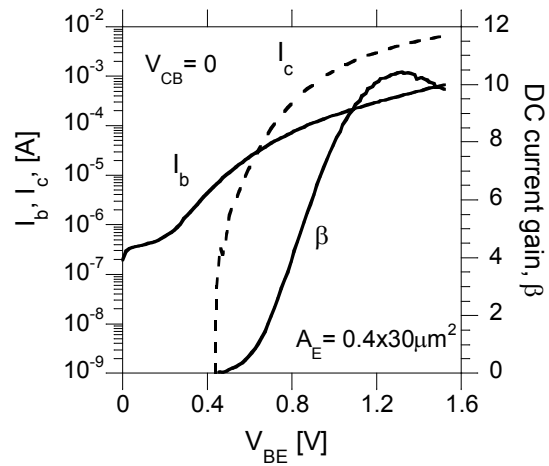


Fig 4: Gummel characteristics in common-base configuration.